

## THIN FILM SENSORS FOR AUTOMOBILE

Yasunori Taga

*TOYOTA Central Research and Development Laboratories, Inc., Nagakute, Aichi 480-11, Japan*

### ABSTRACT

A great amount of effort has been devoted to the constant improvement of such basic performance as drivability, safety and environmental protection. As a result, the total combination of various technologies has made it possible to produce safer and more comfortable automobiles. Among these technologies, plasma and thin film techniques are mainly concerned with sensors, optics, electronics and surface modification. This paper first describes a concept of thin film processing in materials synthesis for sensors based on particle-surface interaction during deposition to provide a long life sensor applicable to automobiles. Some examples of practical application of thin films to sensors are then given. These include (1) a thin film strain gauge for gravity sensors, (2) a giant magneto resistance film for speed sensors, and (3) a Magneto-impedance sensors for detection of low magnetic field.

Further progress of sophisticated thin film technology must be considered in detail to explore advanced thin film materials science and to ensure the field reliability of future sensor devices for automobile.

### INTRODUCTION

The novelty of the functions provided by plasma and thin film technologies, together with their durability for practical use, is emphasized as the area where thin film process has a significant impact. Up to present, thin films have been applied in several fields of applications in several fields of applications in automobile. For example, typical application of thin film sensor in automobile was an oxygen sensor to control the exhaust gas emission of engines. Oxygen sensors have been successfully used in combination with a three-way catalyst system for reducing harmful components in exhaust emission such as hydrocarbon, carbon monoxide and nitro-

gen oxides. Oxygen sensors actually detect the stoichiometric air-fuel ratio in the system. Thin films have also been applied to control the drivability and safety of automobile body and chassis. In fact, various sensors and actuators are used to detect bumps and hollows in the road instantly at high speeds and to make instant responses<sup>[1, 2]</sup>.

It is well known, on the other hand, that the key parts of various sensors are normally made of thin films. For example, speedometers use signals from a vehicle speed sensor to calculate the speed. The cableless vehicle speed sensor, which relies on a magneto-resistance (MR) element, is made of Ni-Co thin films. Practically, this Ni-Co MR film is made on integrated circuit (IC) chips. Another

er example is a thin film type oxygen gas sensor to control exhaust gas emission. Thin films of zirconia ( $ZrO_2+Y_2O_3$ ) are sandwiched by Pt electrodes deposited in turn on porous  $Al_2O_3$  substrate. Various pressure sensors<sup>[2]</sup> are widely used in automobiles, in which thin film sensors for suspension control are included. In this case, Ni alloy films<sup>[3]</sup> are adopted to detect the displacement of diaphragms under low temperature coefficient of resistance (TCR) values less than several ppm.

In practical applications, automobiles are exposed to severe environmental conditions such as high temperature and humidity, and it is therefore important to prepare thin film sensors with reliability and durability for long time usage. So, sophisticated thin film technology plays an important role in thin film preparation of sensors for automobiles. The present author has proposed a new concept of thin film processing for thin film formation<sup>[4,5]</sup>.

This paper first describes a concept of thin film Processing in materials synthesis for sensors based on particle-surface interaction during deposition to provide a long life sensor applicable to automobiles. Some examples of practical applications of thin films to sensors are then given. These include (1) a thin films strain gauge for gravity sensors, (2) a giant magneto resistance film for speed sensors, and (3) a Magneto-Impedance sensors for detection of low magnetic field.

Further progress of sophisticated thin film technology must be considered in detail to explore advanced thin film materials science and to ensure the field reliability of future sensor devices for automobile.

## THIN FILM PROCESS

Irrespective of thin film preparation methods such a Plasma vapor deposition (PVD) and chemical Vapor deposition (CVD), the thin film process comprises three elementary stages, including decomposition, transport, and nucleation and growth<sup>[6]</sup>. Figure 1 shows the flow chart of the thin film process, where starting materials are successively modified to form the resulting film. In the first stage, starting materials in the form of gas, liquid, or solid are decomposed into various fragments of neutrals or ions in the form of atoms, molecules, clusters or powders, by the external powers of plasma, laser, ion, microwave and thermal energies. The decomposed fragments thus formed will travel through the medium of gas or liquid and approach the substrate. This phase is referred to as the transport stage in the thin film process. The Monte Carlo simulation technique is helpful in understanding the mechanism of the transport stage<sup>[7]</sup>. The chemical reaction between the transport medium and the decomposed fragments<sup>[8]</sup> is also important in the reactive process of thin film formation. The decomposed fragments land on the substrate for

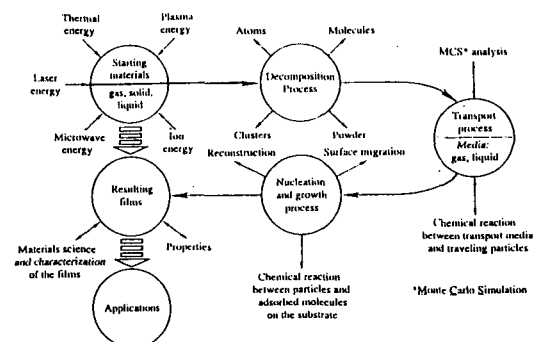


Fig. 1 Flow chart of thin film process

nucleation and growth, which result in the formation of functional films. Thin film properties are strongly influenced at this final stage, because the energy of the decomposed fragments is dissipated in the very shallow surface region of the substrate. This dissipation of the energy of the decomposed fragments may enhance the surface migration of adsorbed atoms, chemical reaction between landing fragments and adsorbed molecules, and finally reconstruction into the structures of the resulting films.

On the other hand, the influence of the kinetic energy of particles in the thin film process<sup>[5]</sup> on thin film formation ranges from simple substrate cleaning for enhanced adhesion to morphological changes and epitaxial growth. Peculiar features of the sputter deposition technique are generally explained in terms of the energy of the sputtered particles which are decomposed and emitted as a result of high energy ion bombardment in the plasma. A complex variety of processes simultaneously occurs whenever energetic particles interact with a substrate or growing films. For a comprehensive description of these processes, the reader is referred to an excellent review in the literature<sup>[9]</sup>. The sputtering process is discussed in view of the energy distribution of sputtered particles and some chemical effects on the substrate surface by high energy ion bombardment.

## APPLICATIONS

### Thin film strain gauge for G sensors

Recent advances in electronics and sensor technologies have been applied to the control functions of the automobile chassis, which

are essential to basic automobile performance. Various sensors and actuators are used to detect bumps and hollows in the road instantly at high speeds and to make instant responses. For example, the active control suspension (ACS) system responds actively to road surface and vehicle running conditions with electronic control of hydropneumatic cylinders. The ACS system receives signals from longitudinal and lateral G sensors<sup>[1]</sup> and consists of a pendulum hung from a thin strip of metal as schematically shown in Fig. 2. Acceleration or deceleration causes the pendulum to swing in the direction of the face, twisting the strip of metal on which amorphous metal strain gauge thin films are deposited to assure reaction stability regardless of the temperature. The most essential requirement for the strain gauge thin film is to have a small value of TCR which can be significantly lowered depending on the thin film preparation conditions<sup>[10]</sup>.

Amorphous Ni-Si-B (NSB) ternary alloy films have been well known for having a high tensile strength (2.6 GPa) and low TCR values ( $10 - 50 \times 10^{-6}/^{\circ}\text{C}$ ) originated from the

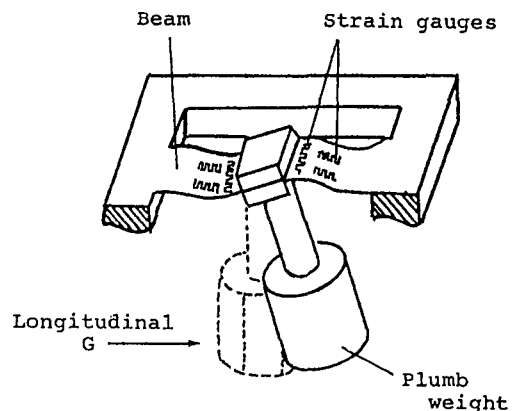


Fig. 2 Schematic illustration of beam structure of the G sensor.

short mean free path (MFP) of electrons in the film.]

In addition, the values of MFP are also recognized to be sensitive to the microstructure of thin films. In the case of sputter deposition, the kinetic energy which is normally determined by energy distribution(ED) of sputtered particles to be deposited gives an important effect on the microstructure of NSB films. From this point of view, the effect of the EDs of sputtered particles on alloy film formation was determined. Two representative sputtering methods used to prepare NSB films were examined; cosputtering with multiple elemental targets of Ni, Si and B (cosputtering), and sputtering with an alloy target of  $\text{Ni}_{67}\text{Si}_{21}\text{B}_{13}$ (alloysputtering). In both sputtering modes, the principal sputtered particles are Ni, Si and B. These particles are detected in the form of ions by secondary ion mass spectrometry (SIMS). These EDs were characterized by the parameters of  $E_m$ (most probable energy), FWHM(full width at half-maximum),  $N$ (tail factor) and  $E_a$  (average kinetic energy). The results are presented in Table 1, where the numerals in parentheses are the values from alloy sputtering. It is worth noting that the  $E_m$  Values of the singly charged monoatomic ions emitted from the alloy were lower than those from the elemental targets. The lowering of the  $E_m$  values resulted in a decrease in the  $E_a$  values of the monoatomic ions. The present results showed that the values of surface binding energy of the atoms in the amorphous alloy target were reduced in comparison with those in the elemental targets. Consequently, the  $E_a$  values of Ni ions formed in the cosputtering mode are very large in comparison with alloy sputtering.

Table 1. Results of the characterization of the energy distributions of sputtered ions.

	Ni <sup>+</sup>	Si <sup>+</sup>	B <sup>+</sup>
$E_m$	1.9(1.5)	2.7(1.9)	2.5(1.5)
FWHM(eV)	7.1(6.9)	10.7(9.8)	13.2(8.6)
$N$	1.6(1.7)	2.0(1.6)	1.4(1.3)
$E_a$	17.1(11.3)	15.5(15.4)	18.4(14.3)

The microstructures of NSB films prepared on NaCl single crystals by cosputtering and alloysputtering modes were examined by means of transmission electron microscopy (TEM). Figure 3 shows TEM images of the films. Obviously, the two films exhibited different microstructures. The cosputtered film showed relatively uniform in low contrast, in which domains of 20 nm in diameter are clearly seen. On the contrary, the alloy sputtered films showed a rather strong contrast and the domain diameter ranged from 5 to 20 nm. The contrast in TEM image could be attributed to mass thickness fluctuation in the film. As a result, it is recognized that the film formed by cosputtering has a more uniform mass thickness than the film formed by alloy sputtering. The TCR values of the cosputtered film were normally less than  $5 \times 10^{-6}/^{\circ}\text{C}$ , but those of

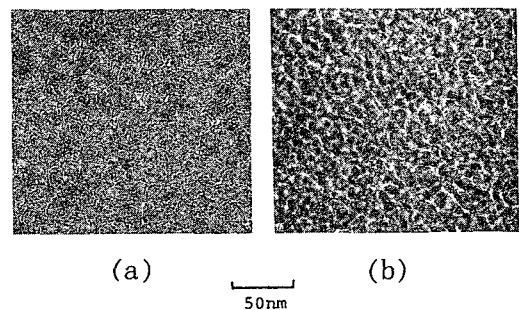


Fig. 3 TEM images of the NSB films prepared by the different deposition methods:(a) alloy sputtering; (b) cosputtering.

alloy sputtering were more  $5 \times 10^{-6}/^{\circ}\text{C}$ . In conclusion, the kinetic energy of depositing particles formed by the sputtering process in a growing film strongly influences the microstructure and electrical property of the resulting films. Typical examples are illustrated by Ni-Si-B amorphous films.

### GMR films for speed sensors

Magnetic principles offer the possibility of the noncontacting measurements of displacement and angle by means of magnetoresistive thin films of NiFe or NiCo. The resistance of the MRE changes according to the magnetic flux changes which occur when the ringed multiple magnet is rotated. The large giant magnetic (GM) value will be therefore advantageous for high sensitive and accurate measurements of displacement and angle.

On the other hand, much attention has been devoted to the giant magnetoresistance (GMR) and antiferromagnetic coupling of several metallic multilayered systems such as Fe/Cr and Co/Cu<sup>[11,12]</sup> instead of NiCo magnetoresistive films. Since the GMR was discovered, its origin has been mainly attributed to the spin-dependent scattering of free electrons at the interface of multilayers. It has been reported that the GMR depends on interfacial roughness, i.e., Co/Cu multilayers with large GM values have atomically rough interfaces, where Co and Cu atoms are distributed randomly<sup>[13,14]</sup>. Judging from these previous studies, we can expect to enhance the value of GM by appropriate modifications of interfacial structures by thin film technology.

A typical example of more detailed investi-

gation GM property, crystallographic structures, and interfacial roughness of magnetron sputtered Co/Cu multilayers deposited on Fe buffer layers with various thickness.

The Co/Cu multilayers were prepared on oxidized Si substrates in a magnetron sputtering system. After deposition of a Fe buffer layer of the thickness,  $t_{\text{Fe}}$ , between 0 and 15 nm, Cu (2.0 nm)/[Co(1.0nm)/Cu(2.0nm)]<sup>16</sup> multilayers were grown at room temperature. The MR was measured by using a conventional four-point geometry. The crystallographic structure of the sample was characterized by X-ray diffraction, and the interfacial atomic structures were evaluated from the distribution of the hyperfine field associated with the Co atoms near interfaces. To obtain the hyperfine field, we have employed NMR measurements of <sup>59</sup>Co in zero field at 4.2 K using a variable frequency spin echo apparatus.

Figure 4 shows the variation of the saturation GM and x-ray diffraction intensity of the (111), (200) and (220) as a function of  $t_{\text{Fe}}$ . A drastic change in the GM was observed at the thickness between  $t_{\text{Fe}}=2.4$  and 3.5nm. In addition, the preferred orientation for the sample is also transformed suddenly from (111) to (110) at the critical Fe buffer thickness of 3.0 nm. There exists a strong correlation between the GM values and their textured structures. Figures. 5(a) and 5(b) are typical examples of the NMR spectra of the samples of  $t_{\text{Fe}} \leq 2.4$  nm and  $t_{\text{Fe}} \geq 3.5$  nm, respectively. It is well known that the tail behind the main peak is attributed to the Co atoms near interfaces. Therefore, the sample of  $t_{\text{Fe}} \leq 2.4\text{nm}$  and  $t_{\text{Fe}} \geq 3.5\text{nm}$  may have not only different crystallinity but also a different in-

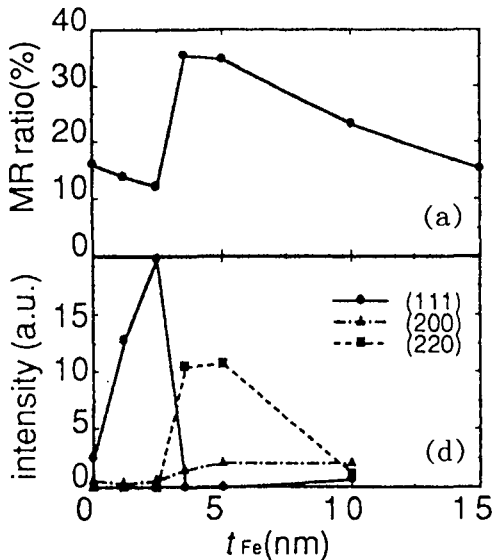


Fig. 4 Variation of (a) MR at 300 K and (b) X-ray diffraction intensity of (111), (200), and (220) of Cu(2.0nm)/[Co(1.0nm)/Cu(2.0nm)]<sup>16</sup> with  $t_{Fe}$ .

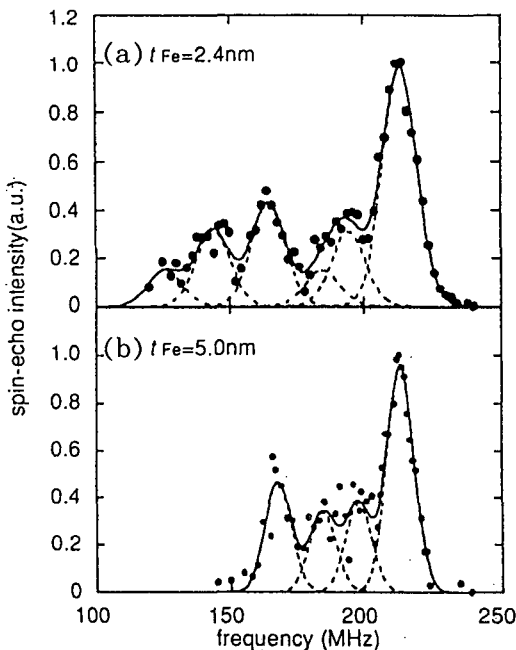


Fig. 5 Typical examples of  $^{59}\text{Co}$  NMR spectra. The thickness of the Fe buffer layer for the samples: (a)  $t_{Fe} \leq 2.4$  nm and (b)  $t_{Fe} \geq 3.5$  nm.

terfacial structure.

In conclusion, the MR values can be modified by controlling the interfacial structures of the Co/Cu multilayers by the sophisticated thin film technology. A strong correlation between the MR values and Co/Cu multilayers with intentionally modified interfaces was revealed NMR analysis. The GMR films of the Cu/Cu multilayer will be influential for the electronic sensor system for the measurement of angular position or angular velocity of the crankshaft or camshaft, of the vehicle wheels.

#### Thin film Magneto-Impedance (MI) sensors

A new type of magnetic sensor based on MI effect<sup>[15]</sup> has been developed to detect low magnetic field. Soft amorphous ferromagnetic wires such as Co-Si-B and Fe-Co-Si-B were first examined and recently thin film type MI sensors became popular. For the purpose of automobile stability control, MI films will be effective for low field ( $\leq 100\text{Oe}$ ) magnetic sensors with high sensitivity. In this section, magnetic properties of layered MI films of the Co-Si-B/Cu/Co-Si-B with magnetic closed - 100p will be presented<sup>[16]</sup>.

A schematic drawing of the Co-Si-B/Cu/Co-Si-B with film is shown in Fig. 6. The films were prepared on Corning glass 7059 with mechanical masks using an rf-magnetron sputtering method, where the target composition was  $\text{Co}_{73}\text{Si}_{12}\text{B}_{15}$ . The sputtering conditions were carefully controlled to make stresses in Co-Si-B film nearly equal to zero. In addition, a constant magnetic field of 100 Oe was applied in parallel to film surface during deposition so as to generate uniaxial anisotropy in the magnetic layers. As a result,

the easy axis was set in the transverse direction of the films.

Typical example of waveforms of the voltage  $V$  of the MI film was shown in Fig. 7, where large change in voltage can be seen between with and without external magnetic fields. Voltage change ratio  $\Delta V/V$  was calculated to be 140%. Figure 8 represents the changes in inductance  $L$  and resistance  $R$  as

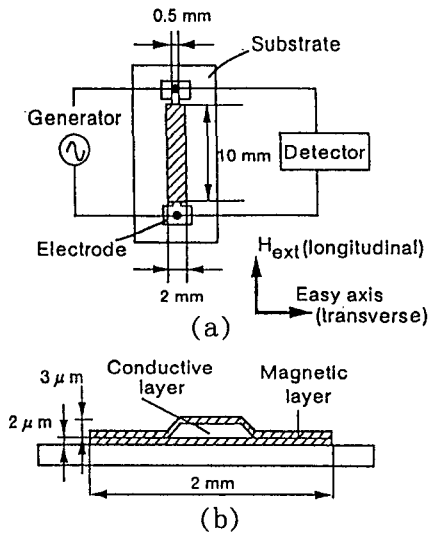


Fig. 6 Schematic drawing of the layered GMI element and measurement system: (a) top view; (b) cross-sectional view.

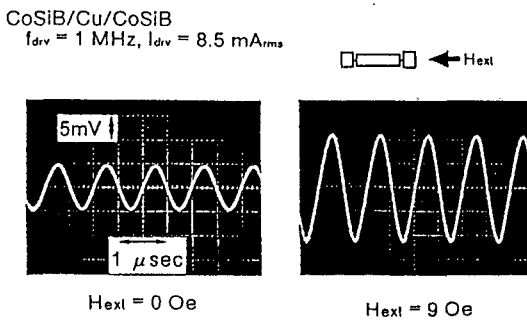


Fig. 7 Waveforms of the voltage  $V$  of the CoSiB/Cu/CoSiB element at  $H_{ext}=0$  Oe and  $H_{ext}=9$  Oe. The driving current was 8.5 mA and the frequency was 1 MHz.

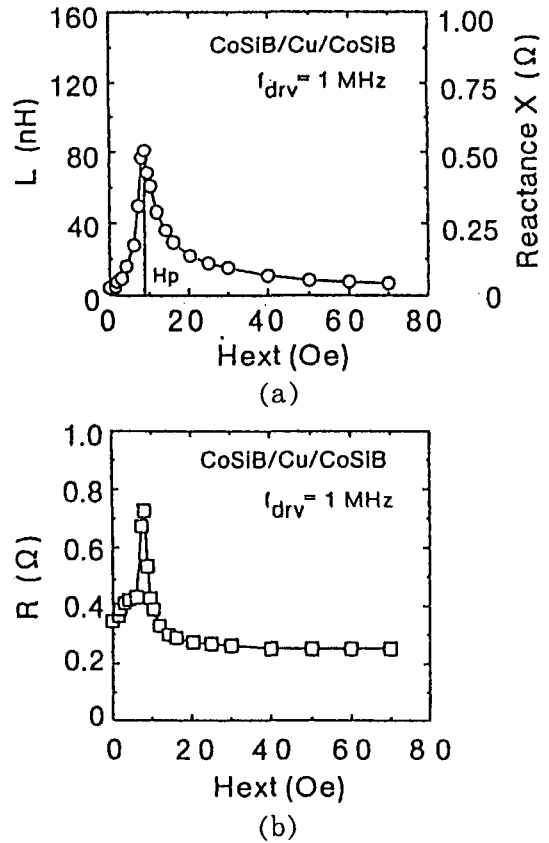


Fig. 8 Dependence of (a) the inductance  $L$  and (b) the resistance  $R$  on the external field  $H_{ext}$ .

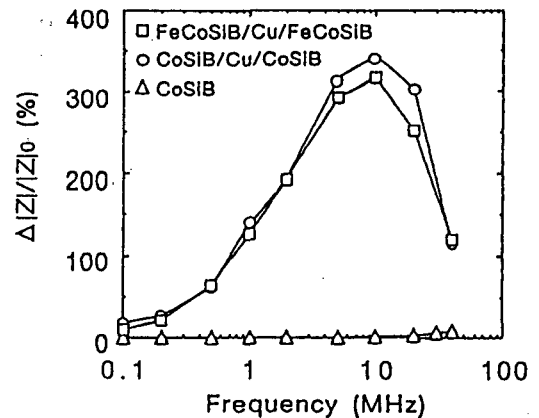


Fig. 9 Dependencies of the impedance change ratio on the ac driving frequency for CoSiB/Cu/CoSiB, FeCoSiB/Cu/FeCoSiB, and CoSiB films.

a function of the external field  $H_{ext}$ .  $L$  and  $R$  show same maximum at 9 Oe of  $H_{ext}$ . ( $= H_p$ ). As for the content of the impedance  $|Z|$ , the ratio of the reactance  $X$  to the resistance  $R$  are 1:1 and therefore, large contribution of the resistance  $R$  is estimated in thin film MI sensors. In conclusion, the values of the impedance change ratio  $\Delta Z/Z$  are more than 300%/9Oe at 10MHz and the sensitivity is 35%/Oe(Figure 9). This type of high performance magnetic sensor will be considered for application in various industrial fields.

### CONCLUSION

State of the art of thin film technology in automobile sensors has been reviewed. It has become possible to control thin film nanostructure by taking thin film and ion-solid interaction process into consideration. Durability and reliability of thin film sensors for practical application to automobiles were particularly emphasized with sophisticated thin film preparation techniques. Several examples were presented to elucidate the relationship between thin film structures and sensor properties. Finally, further challenges to applications of thin film technology to the development of sensors in automobiles are now in progress.

### REFERENCES

1. F. Heintz and E. Zabler, SAE Technical Paper NO. 870477 (1987).
2. Y. Taga, J. Vac. Sci. Technol. A13, 990 (1995).
3. H. Yamadera and Y. Taga, Appl. Phys. Lett. 55, 1080 (1989).
4. Y. Taga, MRS Symp. Proc. 268, 95 (1992).
5. Y. Taga, R & D Review of TOYOTA CRDL 28, 1 (1993).
6. Y. Taga, Proc. Soc. Photo-Opt. Instrum. Eng. 1275, 10 (1990).
7. T. Motohiro and Y. Taga, Thin Solid Films 112, 161 (1984).
8. T. Ohwaki and Y. Taga, Nucl. Instrum. Methods Phys Res. B33, 523 (1988).
9. P. J. Martin, J. Mater. Sci. 21, 1 (1986).
10. Y. Taga and Y. Gotoh, Thin Solid Films 193, 164 (1990).
11. M. N. Baibich, J. M. Broto, A. Fert, F. Nguyen Van Dau, F. Petroff, P. Etienne, G. Creuzet, A. Friedrich and J. Chazelas, Phys. Rev. Lett. 66, 2152 (1991).
12. S. S. P. Parkin, R. Bhada, and K. P. Roche, Phys. Rev. Lett 66, 2152 (1991).
13. M. Suzuki, Y. Taga, A. Goto and H. Yasuoka, Phys. Rev. B50, 18/580(1994).
14. M. Suzuki, Y. Taga, Phys. Rev. B52, 361 (1995).
15. L. V. Panina and K. Mohri, Appl. Phys. Lett. 65, 1189 (1994).
16. T. Morikawa, Y. Nishibe, H. Yamadera, Y. Nonomura, M. Takeuchi, J. Sakata and Y. Taga, IEEE Trans. on Magnetics, in press.